Supplementary Information

1. **Expanded Methods (Materials and Methods Tables 1–4)**
2. **Supplementary Figures 1–13**
3. **Supplementary Table 1**

Expanded Materials and Methods

Materials and Methods Table 1. Sequence of sgRNA, HDR donor template, and PCR primers.

sgRNA sequence			
TTCTAATACGACTCACTATAGGGCGCTCACCCTCGCATTGGTTTTAGAGCTAGA			
HDR donor template sequence			
CCGCTGGGACCCGCGAGCCCCGCCGCCGTTATGAACATCAGCAATGCGAGGGTGAGC GCCCGAAGCGGGAGGCTGTCCGCGCCGCGTGG			
PCR primers for amplifying the off-target loci			
#	Off-target position	Forward primer	Reverse primer
1	Chr2:129374717	CAGTGCTGAGTGAAGGCAGA	CCTCTCTGAATTTGGGCCGTC
2	Chr11:1492482	ATGAGCGGCAGAAACCAAGA	GCAGCACGCACTTGTGTAAAC
3	Chr17:75243875	GCAGGGCGATGTTTTAGCAG	CAGCATCTTCCTTGGAGGGGC
4	Chr8:59491100	GTCTTGCAGTTGTGTGGTGC	GAAAGGGAGGCATGCAGCTAT
5	ChrX:100869663	TGCCATGGCTTTAGGGAAGG	CCGGCACAGAGAAATCCCTTC

Materials and Methods Table 2. Single-cell electrophysiology recording conditions.

	AP	I_{Na}	I_{CaL}	I_{Ks}	I_{Kr}
Configuration	Current clamp	Voltage clamp	Voltage clamp	Voltage clamp	Voltage clamp
Sampling rate (kHz)	50	100	50	10	10
Filter (kHz)	10	20	10	1	1
Temperature (°C)	35 ± 1	20 ± 1	34 ± 1	34 ± 1	34 ± 1
Perforated /Ruptured	Perforated	Ruptured	Perforated	Ruptured	Ruptured

Patch Clamp Extracellular Solution (mM)						
	AP	I_{Na}	I_{Na}-Late	I_{CaL}	I_{Ks}	I_{Kr}
NaCl	150	70	150	140	150	150
NMDG		70		-		
KCl	5.4	-	5.4	-	5.4	5.4
$CsCl_2$		5.4		10		
$CaCl_2$	1.8	1.8	1.8	1.8	1.8	1.8
$MgCl_2$	1	1.2	1	1	1	1
Glucose	15	10	15	10	15	15
HEPES	15	10	15	10	15	15
Na-Pyruvate	1	2	1	-	1	1
Nifedipine	-	0.01	0.01	-	0.002	0.002
E4031	-	-	-	-	0.001	-
pH 7.4	NaOH	HCl	NaOH	NaOH	NaOH	NaOH

Patch Clamp Intracellular Solution (mM)					
	AP	I_{Na} / I_{Na}-Late	I_{CaL}	I_{Ks}	I_{Kr}
KCl	150	-	-	20	150
L-Aspartic Acid	-	120	-	-	-
$CsCl_2$	-	20	120	-	-
CsOH	-	120	-	-	-
NaCl	5	-	-	-	5
$CaCl_2$	2	-	-	-	2
EGTA	5	10	10	10	5
HEPES	10	10	5	5	10
MgATP	5	-	5	5	5
Na2-ATP	-	4	-	-	-
K-Aspartate	-	-	-	125	-
$MgCl_2$	-	2	-	1	-
Na_2-Phosphocreatine	-	-	-	2	-
Na_2-GTP	-	-	-	2	-
Escin	0.025	-	0.025	-	-
pH	7.2 (NaOH)	7.3 (CsOH)	7.2 (CsOH)	7.2 (NaOH)	7.2 (NaOH)

Materials and Methods Table 3. Antibodies used in this study.

Primary antibodies			
Antigen	Manufacturer	Catalog number	Concentration
NAA10	Atlas antibodies	HPA030711	1:1000 (WB)
ARD1A	Proteintech	I4803-I-AP	1:3000 (WB)
NAA15	Atlas antibodies	HPA023589	1:1000 (WB)
Vinculin	Santa Cruz	sc-73614	1:200 (WB)
β-Actin	Cell Signaling Technology	3700	1:1000 (WB)
SCN5A	Alomone labs	ASC-005	1:500 (WB)
DDDDK tag (FLAG tag)	Abcam	ab1257	1:1000 (WB)
Transferrin receptor	Invitrogen	13-6800	1:1000 (WB)
RyR2	Badrilla	A010-35AP	1:1000 (WB)
SERCA	Santa Cruz	sc-376235	1:100 (WB)
NCX1	Alomone labs	ANX-011	1:500 (WB)
PLN	Cell Signaling Technology	14562	1:1000 (WB)
α-Actinin (Sarcomeric) (FITC-conjugated)	Miltenyi Biotec	130-119-766	1:50 (IF)
Phalloidin (Alexa647-conjugated)	Invitrogen	A22287	1:400 (IF)
WGA (Alexa647-conjugated)	Invitrogen	2126807	1:1000 (IF)
cMyc (Alexa647-conjugated)	BioLegend	626810	1:100 (IF)
Secondary antibodies			
HRP goat anti-mouse IgG	Bio Rad	51782504	1:10000 (WB)
HRP donkey anti-rabbit IgG	Bio Rad	644005	1:10000 (WB)
IRDye800 CW donkey anti-mouse	LI-COR Biosciences	926-32212	1:10000 (WB)
IRDye680 RD donkey anti-goat	LI-COR Biosciences	926-68074	1:10000 (WB)
Alexa647 donkey anti-rabbit	Invitrogen	A32795	1:1000 (IF)
Hoechst 33258	Molecular Probes	H-3569	1:500 (IF)

IF: immunofluorescence, WB: western blot

Materials and Methods Table 4. Parameter settings for analysis of mass spectrometry data.

COMET	
Isotope error = type 3; Fragment bin tolerance = 0.2; Fragment bin offset = 0; Theoretical fragment ions = 0	
HYTANE Nt-acetylation	Enzyme number = 5 (ArgC); Digestion type = Semi; Missed cleavage = 2; Fixed modification: C_cysteine = 57.021464, K_lysine = 28.0313; Variable modification: variable_mod01 = 15.9949 M 03-100, variable_mod02 = 42.010565 n 01-101, variable_mod03 = 6.031817 K 03-100
LATE Nt-acetylation	Enzyme number = 4 (LysN); Digestion type = Semi; Missed cleavage = 0; Fixed modification: C_cysteine = 57.021464; Variable modification: variable_mod01 = 15.9949 M 03-100, variable_mod02 = 42.010565 n 01-101
XPRESS	
Mass tolerance = 20 ppm; The minimum number of chromatogram points needed for quantification = 3; The number of isotopic peaks to the sum = 0	

a

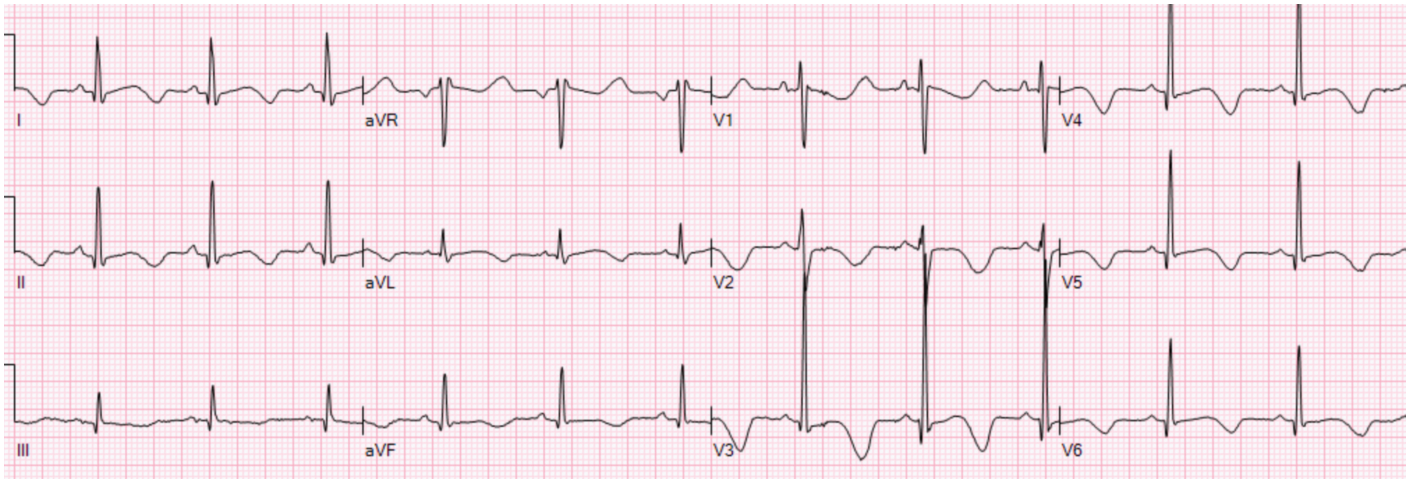

b

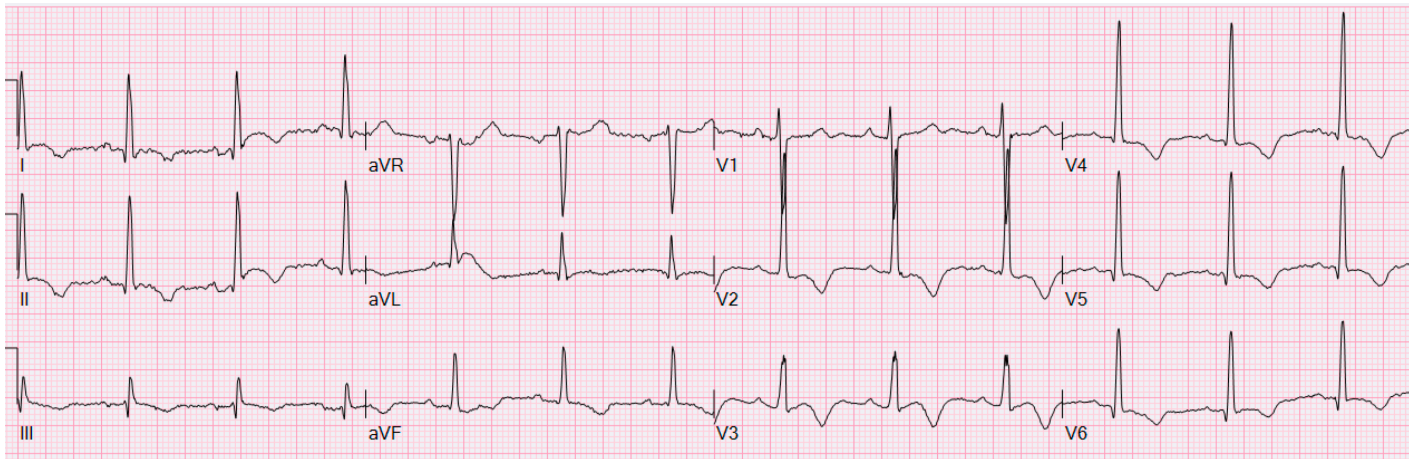

c

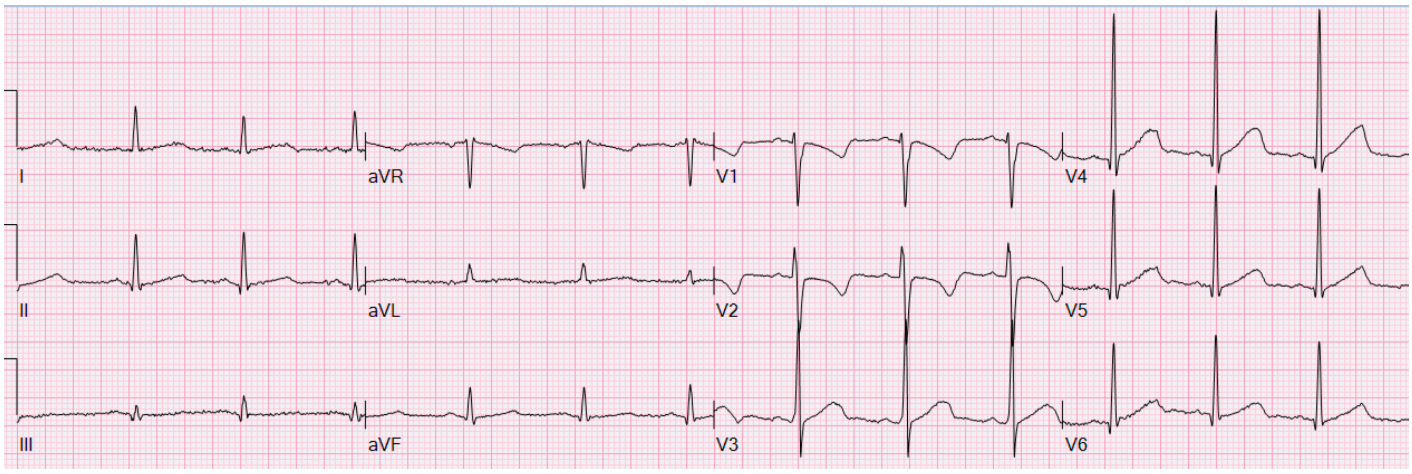

Supplementary Figure 1. QT prolongation and T-wave abnormalities in patients with the NAA10-R4S variant. A. ECG for patient III:8 demonstrates T-wave inversions and QT prolongation (QTc = 545 msec). **B.** ECG for patient III:1 demonstrates T-wave inversions, possible LVH, and QT prolongation (QTc = 491 msec). C. ECG for patient IV:4 demonstrates QT prolongation (QTc = 515 msec). All ECGs were recorded at a standard paper speed of 25 mm/sec and 10 mm/mV, with a high-pass filter at 0.05 Hz and a low-pass filter at 150 Hz.

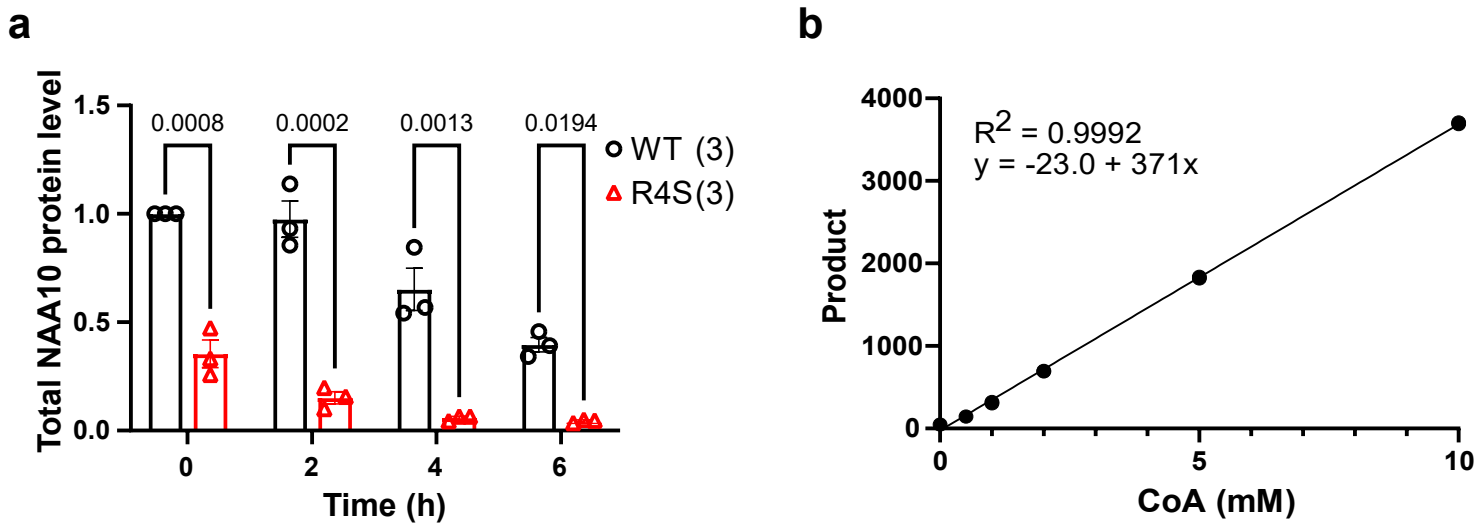

Supplementary Figure 2. Biochemical analysis of NAA10 p.R4S. a. After administration of cycloheximide to inhibit protein translation, the NAA10 protein was measured by a specific antibody and normalized to vinculin (three biological replicates; p = 0.0338; two-way ANOVA). **b.** Increasing concentrations of coenzyme A (CoA) were added to the solution containing ThiolGlo4, and the resulting fluorescence (Ex = 400 nm, Em = 465 nm) was quantified in a plate reader. A linear fit was calculated.

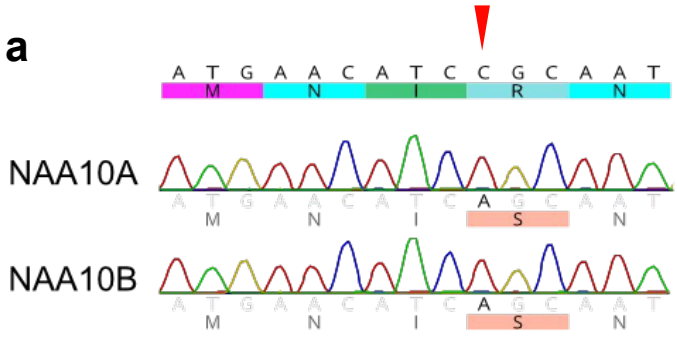

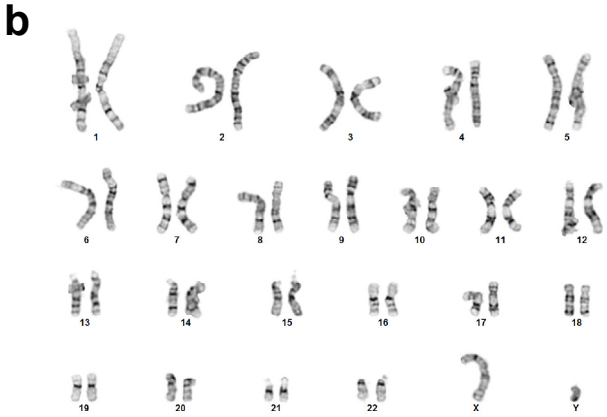

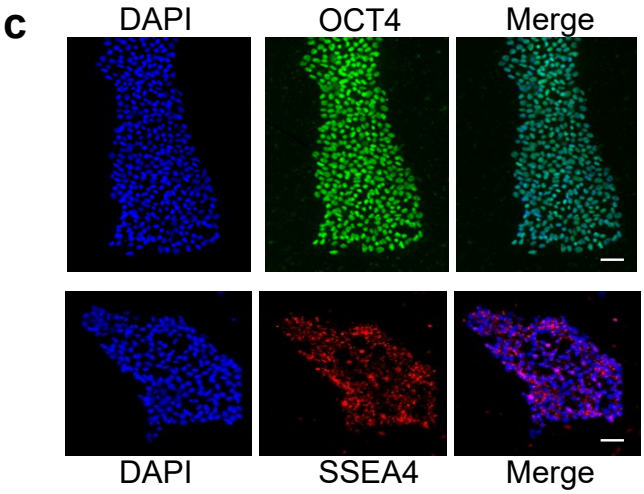

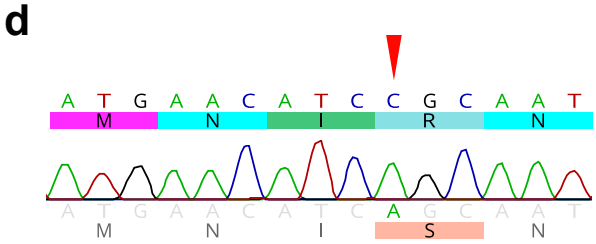

e

CFD Spec. Score	R4 SITE ON-TARGET SEQUENCES			SEQUENCING RESULTS
98	chrX:153200326-153200348:-	Exon	gRNA-NAA10	GGGCGCTCACCCTCGCATTGCGG

#	CFD off-target score	R4 SITE OFF-TARGET SEQUENCES			SEQUENCING RESULTS
1	0.240625	chr2:129374718-129374740:+	Intergenic	AC012451.1-AC068483.1	No mutations
2	0.147636	chr11:1492483-1492505:-	Intron	MOB2	No mutations
3	0.136878	chr17:75243876-75243898:-	Intergenic	SEC14L1-RP11-285E9.6	No mutations
4	0.121008	chr8:59491101-59491123:-	intron	SDCBP	No mutations
5	0.099310	chrX:100869664-100869686:-	intergenic	RP4-545K15.3-ARMCX6	No mutations

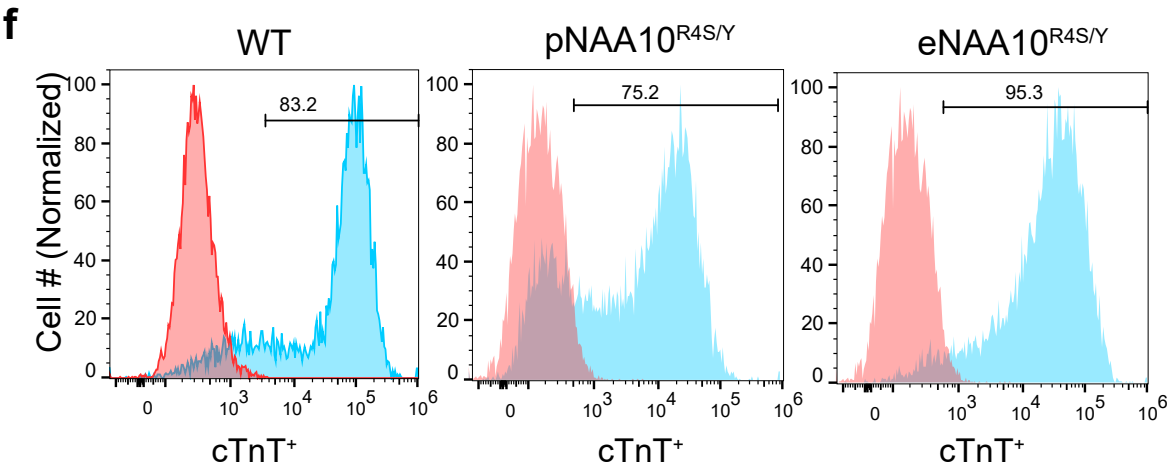

Supplementary Figure 3. Characterization of patient-derived iPSCs with NAA10 p.R4S variants. a. Sanger sequencing of two independent clones for the NAA10 p.R4S identified after somatic cell reprogramming of peripheral blood mononuclear cells (PBMCs) from a male patient with NAA10-related syndrome. **b.** G-banding of clone NAA10A demonstrated a normal male karyotype, designated as pNAA10R4S/Y. **c.** Micrographs of iPSC colonies fixed and stained with pluripotency markers, OCT4 and SSEA4. Scale bar: 100 µm. **d.** Sanger sequencing of the genome-edited line designated as eNAA10R4S/Y. **e.** Sequencing of off-target sites in the eNAA10R4S/Y clone did not reveal any genetic abnormalities. **f.** Differentiated iPSC-CMs were isolated as single cells, stained with an antibody against cardiac troponin-T coupled to FITC, and quantified by flow cytometry (blue traces). Traces in red were from unstained cells. The percentage of cTnT+ iPSC-CMs is listed on the graphs.

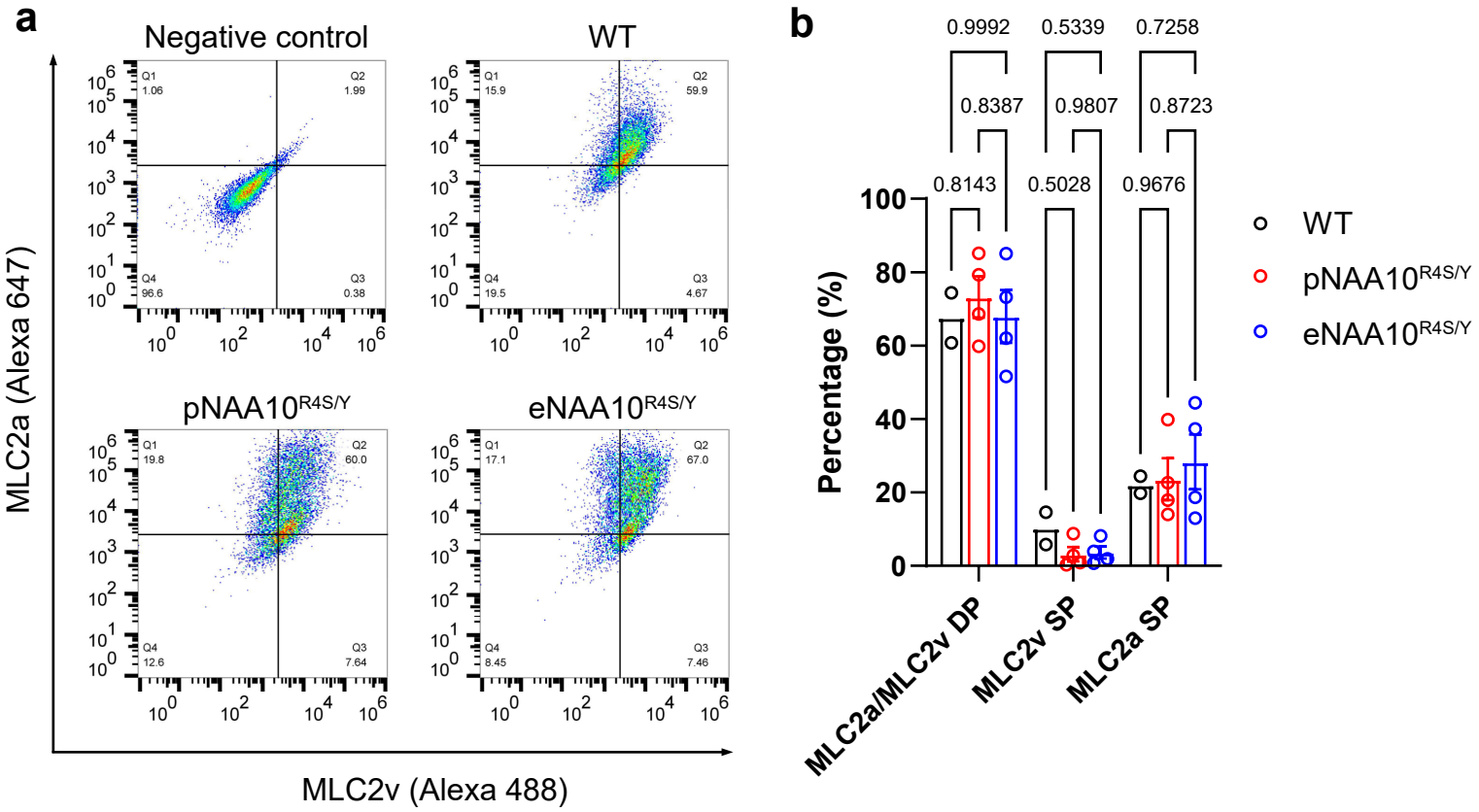

Supplementary Figure 4. Cell fractions based on MCL2a and MCL2v expression in iPSC-CMs. a. Representative dot plots showing MCL2a and MCL2v expression in iPSC-CMs. **b.** Quantification of the population of MCL2a single-positive (SP) cells, MCL2v SP cells, and MCL2a/MCL2v double-positive (DP) cells. There was no significant difference in the population (n = 2, 4, and 4, independent differentiation experiments in WT, pNAA10$^{R4S/Y}$, and eNAA10$^{R4S/Y}$, respectively; p = 0.8555; two-way ANOVA).

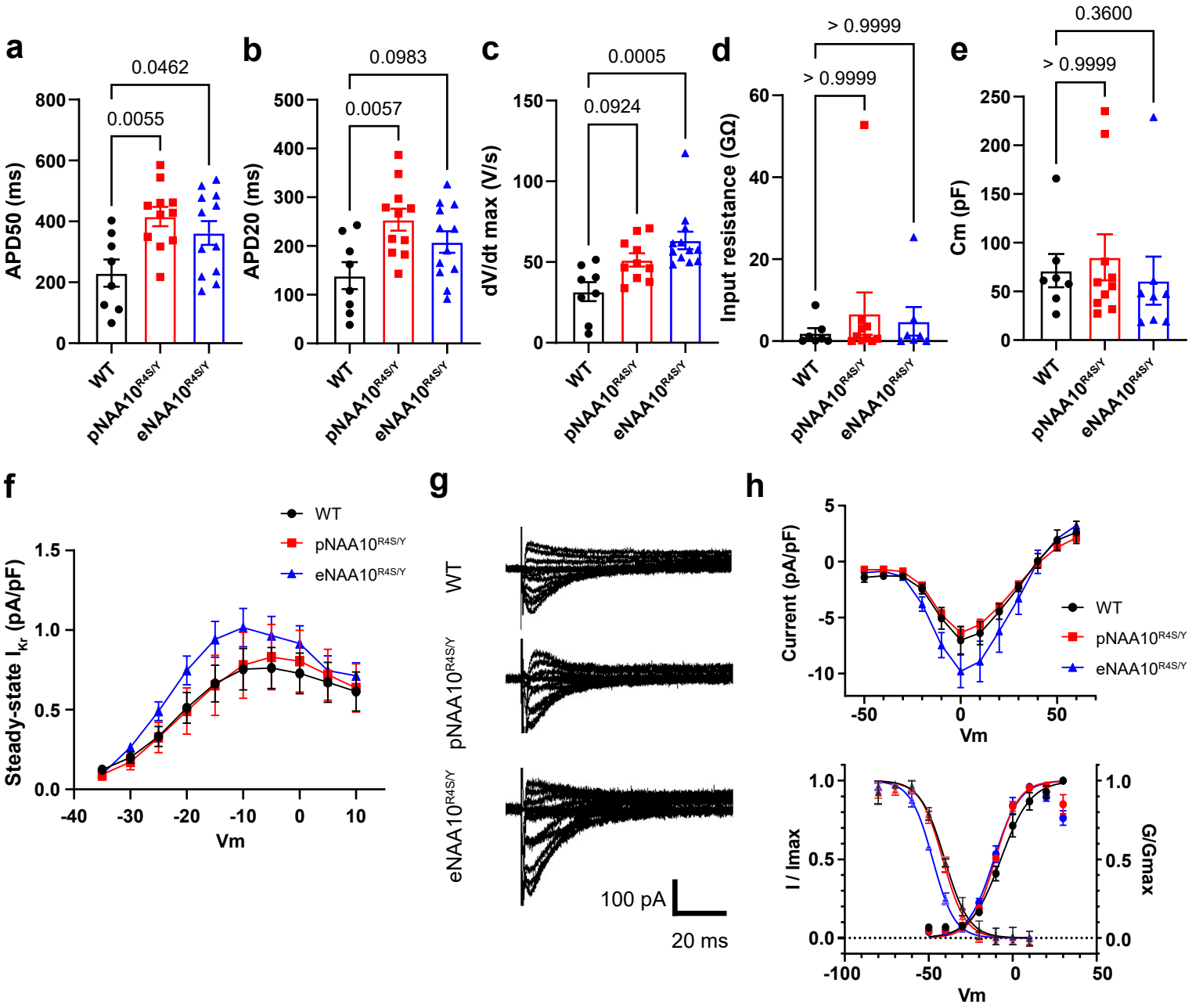

Supplementary Figure 5. Electrophysiological analysis of NAA10$^{R4S/Y}$-iPSC-CMs. a. APD50 demonstrates significant prolongation in both pNAA10$^{R4S/Y}$- and eNAA10$^{R4S/Y}$-iPSC-CMs compared to WT-iPSC-CMs (230.3 ± 44.4 ms, 416.1 ± 31.6 ms, and 362.1 ± 39.1 ms; p = 0.0101; one-way ANOVA). **b.** APD20 demonstrates significant prolongation in both pNAA10$^{R4S/Y}$-iPSC-CMs while eNAA10$^{R4S/Y}$-iPSC-CMs did not show statistical significance compared to WT-iPSC-CMs (139.2 ± 27.6 ms, 253.9 ± 22.4 ms, and 208.2 ± 22.2 ms; p = 0.0115; one-way ANOVA). **c.** eNAA10$^{R4S/Y}$-iPSC-CMs demonstrated larger dV/dt max. pNAA10$^{R4S/Y}$-iPSC-CMs also showed a tendency toward a larger dV/dt max though statistical significance was not seen (31.7 ± 5.9 V/s, 51.3 ± 4.1 V/s, and 63.4 ± 5.5 V/s; p = 0.0013; Kruskal-Wallis test). **d.** No statistically significant difference was seen in input resistance (2.0 ± 1.2 GΩ, 6.7 ± 5.1 GΩ, and 4.8 ± 3.5 GΩ; p = 0.8961; Kruskal-Wallis test). **e.** Membrane capacitance (Cm) had no significant difference among the three groups (71.4 ± 17.1 pF, 85.1 ± 23.7 pF, and 61.0 ± 24.7 pF; p = 0.3138; Kruskal-Wallis test). For a–e, the same cells were analyzed. n = 8, 11, and 12, independent experiments; n = 7, 6, 7, independent differentiation experiments in WT-, pNAA10$^{R4S/Y}$-, eNAA10$^{R4S/Y}$-iPSC-CMs, respectively. **f.** There was no significant difference in steady-state I_{Kr} (n = 6, 7, and 7, independent experiments; n = 3, 3, 3, independent differentiation experiments in WT-, pNAA10$^{R4S/Y}$-, eNAA10$^{R4S/Y}$-iPSC-CMs, respectively; p = 0.6512; two-way repeated measures ANOVA). **g.** Representative traces of I_{CaL} from control, pNAA10$^{R4S/Y}$-, and eNAA10$^{R4S/Y}$-iPSC-CMs. **h.** Current-voltage relation of normalized whole-cell I_{CaL} with no significant difference in either pNAA10$^{R4S/Y}$- or eNAA10$^{R4S/Y}$-iPSC-CMs (upper panel) (p = 0.1947; two-way repeated measure ANOVA). I_{CaL} normalized with maximal conductance and maximal current density represent voltage-dependent activation and inactivation curves respectively (lower panel) (n = 3, 8, and 6, independent experiments; n = 3, 3, 3, independent differentiation experiments in WT-, pNAA10$^{R4S/Y}$-, eNAA10$^{R4S/Y}$-iPSC-CMs).

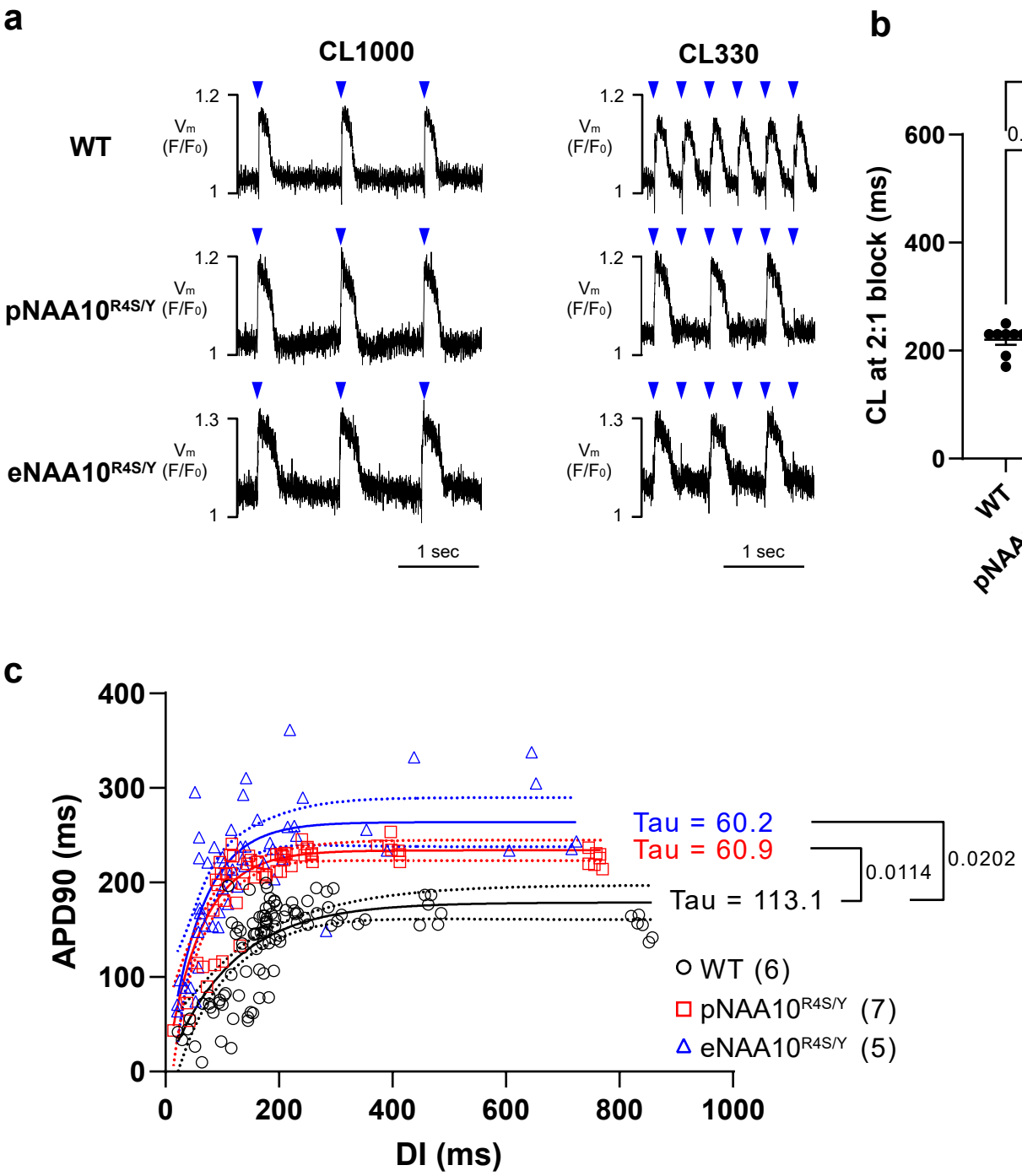

Supplementary Figure 6. APD restitution was steeper in pNAA10$^{R4S/Y}$ and eNAA10$^{R4S/Y}$ compared to WT. a. iPSC-CMs were electrically stimulated with the standard dynamic method, in which starting with a cycle length (CL) of 1000ms, the CL was progressively decreased until 2:1 block occurred. Arrowheads indicate electrical stimulation. **b.** The CL at 2:1 block was significantly longer in pNAA10$^{R4S/Y}$ and eNAA10$^{R4S/Y}$ compared to WT (WT: 220.0 ± 9.3 ms vs pNAA10$^{R4S/Y}$: 297.3 ± 19.8 ms, and eNAA10$^{R4S/Y}$: 336.0 ± 29.3 ms; mean ± SEM; n = 8, 11, 10, independent experiments; p = 0.0076; Kruskal-Wallis test). **c.** The restitution curve was fitted to a mono-exponential function: APD = APD_{stable} * (1- b*exp(-DI*K)), where the time constant (Tau) is 1/K. Differences in K between pNAA10$^{R4S/Y}$ vs WT, and eNAA10$^{R4S/Y}$ vs WT, were tested using extra sum-of-squares F test. n = 6, 7, 5, independent experiments in WT, pNAA10$^{R4S/Y}$, and eNAA10$^{R4S/Y}$, respectively. CL: cycle length, DI: diastolic interval.

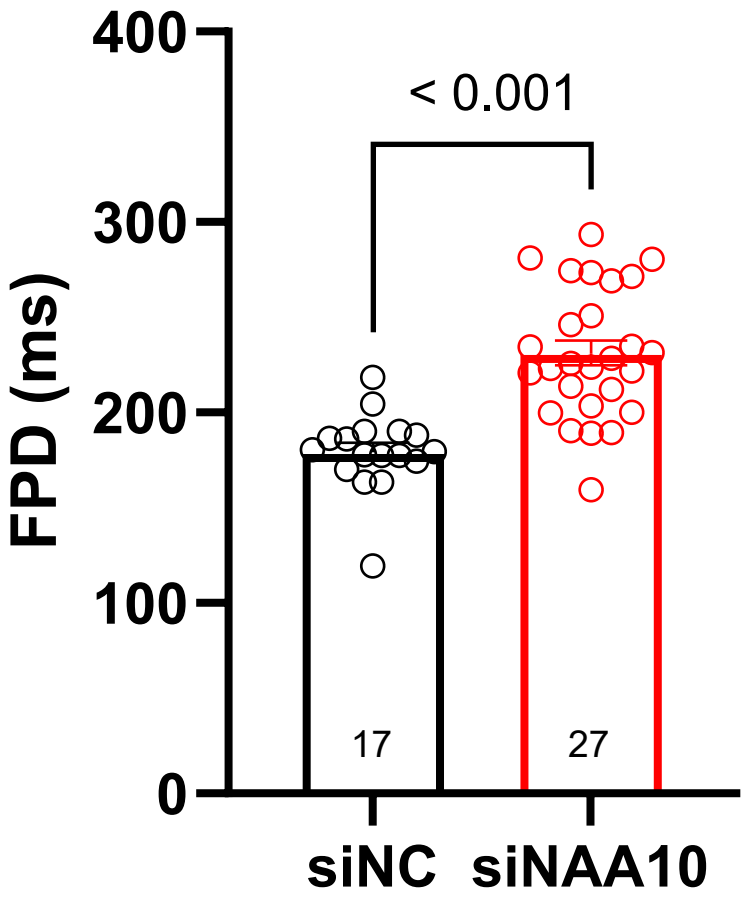

Supplementary Figure 7. NAA10 knockdown caused FPD prolongation. NAA10 was knocked down using siRNA in WT-iPSC-CMs, and FPD was measured 2 days after transfection. FPD was prolonged in WT-iPSC-CMs with NAA10 knockdown (231.3 ± 6.6 ms vs 179.3 ± 5.0 ms; mean ± SEM). Statistical analysis was conducted using two-tailed unpaired t-test.

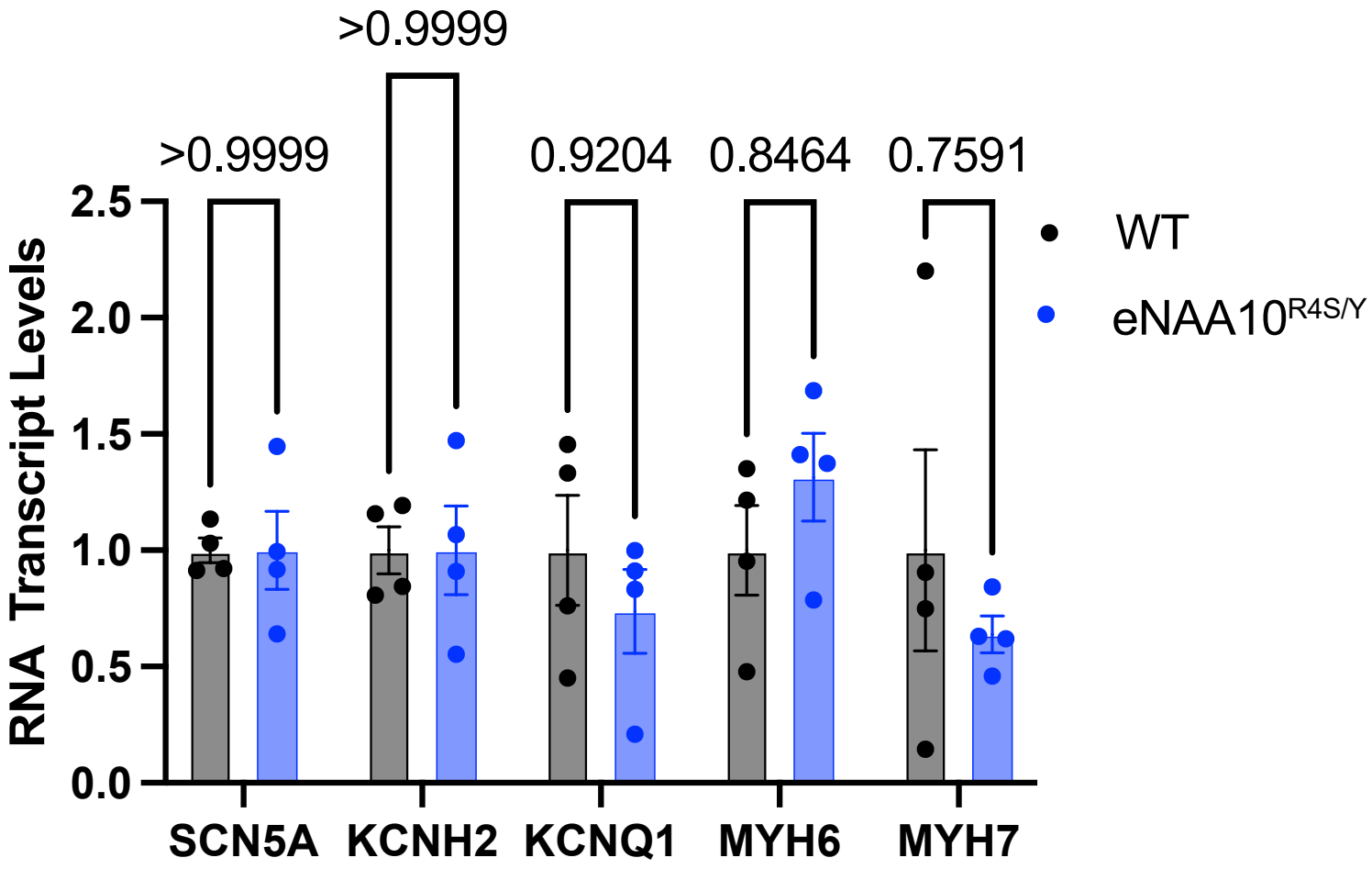

Supplementary figure 8. NAA10 dysfunction does not cause transcriptional changes in major ion channels or structural genes. Whole RNA isolated from WT- and eNAA10$^{R4S/Y}$-iPSC-CMs was analyzed by quantitative PCR with gene-specific primers (mean ± SEM; n = 4, biological replicates). Statistical analysis was performed using two-way ANOVA; p-values are listed.

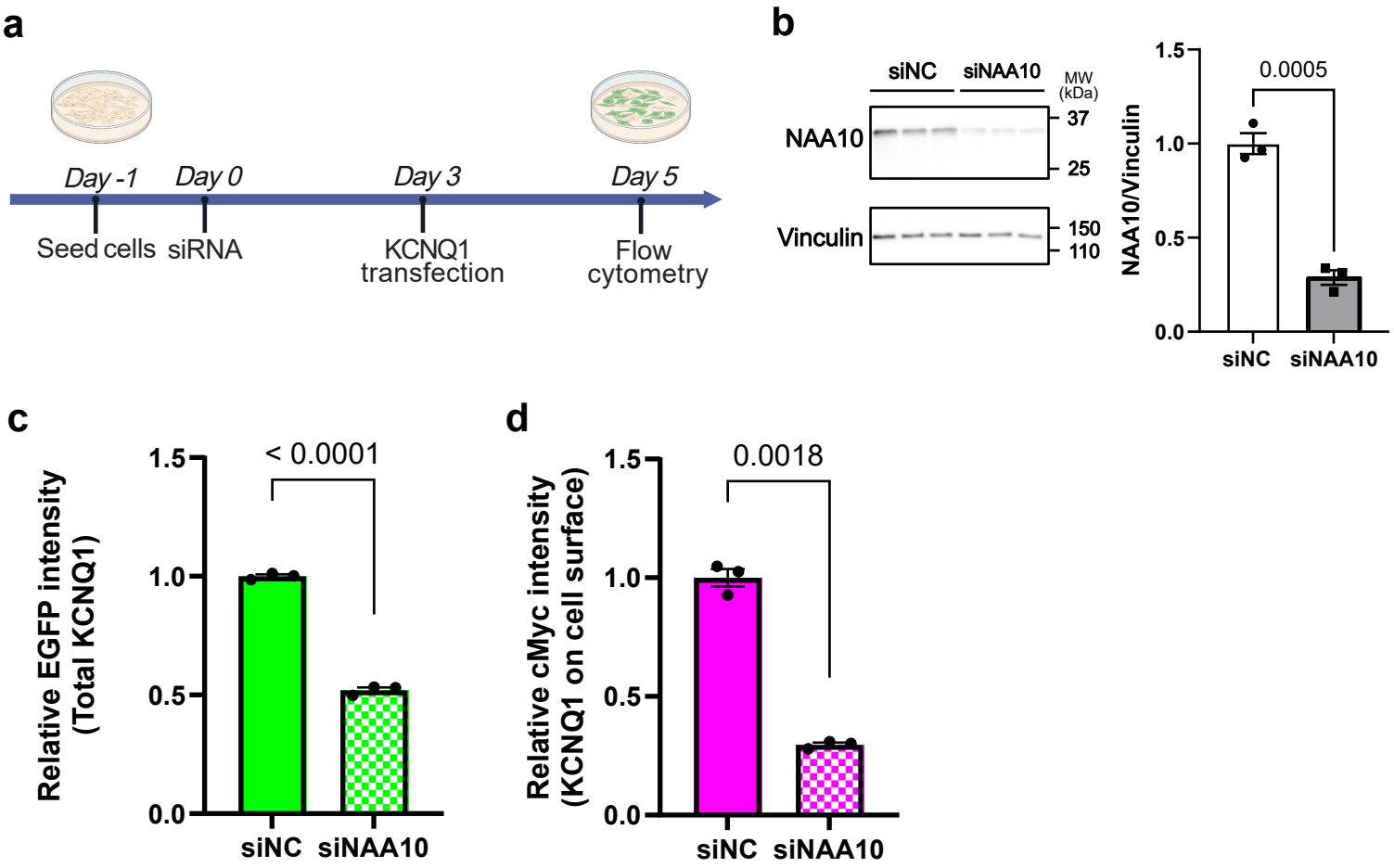

Supplementary Figure 9. NAA10 knockdown reduced KCNQ1 level on the cell membrane. a. Timeline of siRNA and KCNQ1 transfection in HEK cells. Created in BioRender. Yoshinaga, D. (2025) https://BioRender.com/k75h424. **b.** NAA10 was successfully knocked down by siRNA. (siNC = 1.0 ± 0.06 vs siNAA10 = 0.3 ± 0.04; n = 3, biological replicates; two-tailed unpaired t-test). **c.** The geometric mean of EGFP intensity in EGFP-positive cells was measured and the value was normalized with the intensity of siNC (1.0 ± 0.01 vs 0.5 ± 0.01; mean ± SEM; n = 3, biological replicates). **d.** The geometric mean of cMyc-Alexa647 intensity in EGFP-positive cells was measured, and the value was normalized with the intensity of siNC (1.0 ± 0.04 vs 0.3 ± 0.01; mean ± SEM; n = 3, biological replicates). Statistical analysis was performed by two-tailed unpaired t-test.

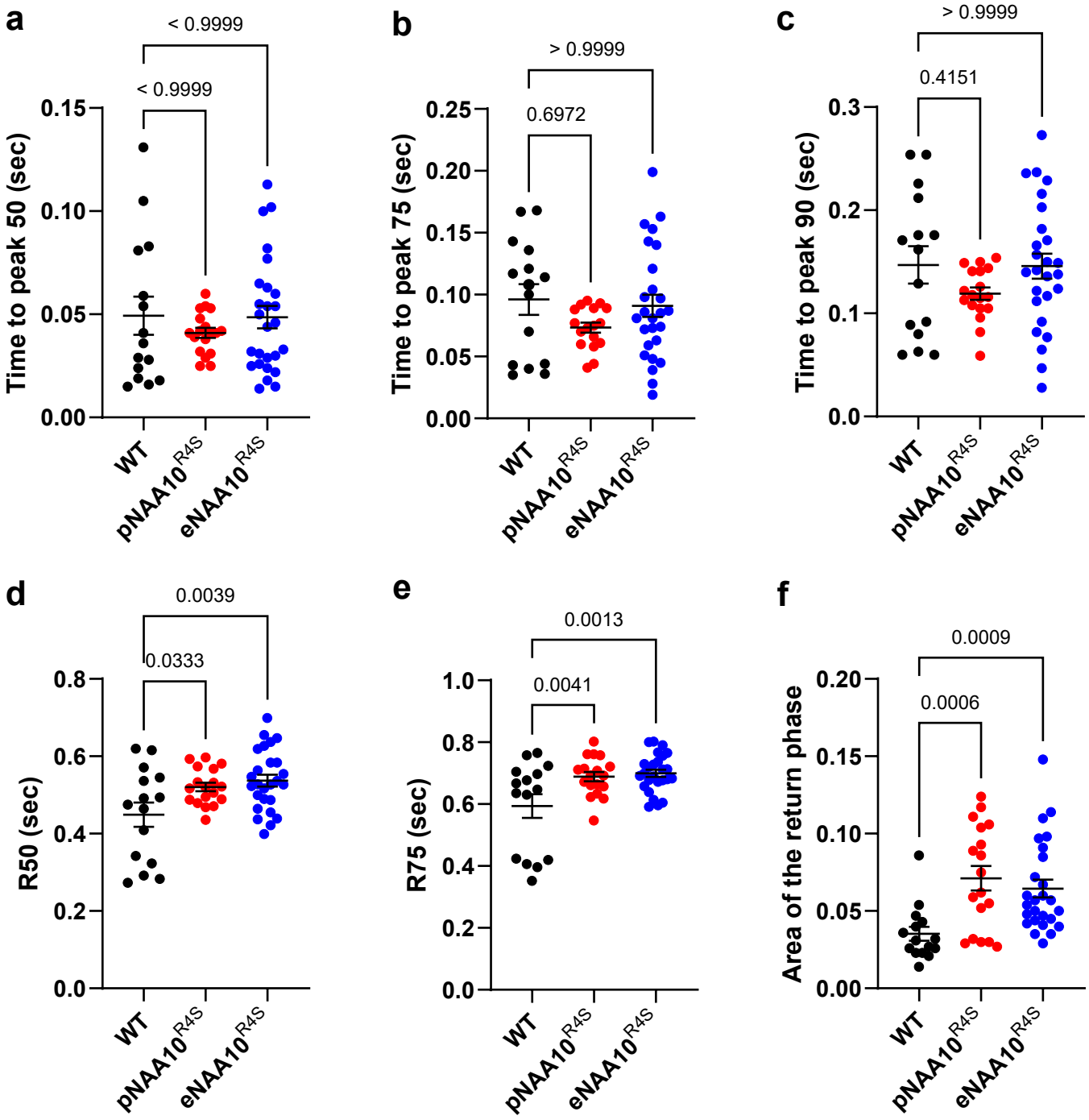

Supplementary Figure 10. Ca^{2+} reuptake is disrupted in NAA10$^{R4S/Y}$-iPSC-CMs. a–c. Parameters indicating the speed of Ca^{2+} elevation, such as Time to peak 50 (**a**), 75 (**b**), and 90 (**c**), were not altered. ($p > 0.05$; Kruskal-Wallis test). **d, e.** The time to 50% and 75% of the baseline (R50 and R75) was prolonged in NAA10$^{R4S/Y}$-iPSC-CMs, indicating Ca^{2+} reuptake is disrupted. (R50, WT: 0.45 ± 0.03 sec vs. pNAA10$^{R4S/Y}$: 0.52 ± 0.01 sec, and eNAA10$^{R4S/Y}$: 0.54 ± 0.02 sec; R75, WT: 0.59 ± 0.04 sec vs. pNAA10$^{R4S/Y}$: 0.69 ± 0.01 sec, and eNAA10$^{R4S/Y}$: 0.70 ± 0.01 sec; mean ± SEM; n = 15, 18, and 26, independent experiments; three independent differentiation experiments; $p = 0.0069$, and 0.0018, respectively; one-way ANOVA). **f.** The area of the return phase ($Area_{ret}$), which is an integration of the values under the curve from peak to the end of the transient, is an alternative parameter of Ca^{2+} re-uptake. Both pNAA10$^{R4S/Y}$ and eNAA10$^{R4S/Y}$ demonstrated larger $Area_{ret}$, indicating disrupted Ca^{2+} reuptake in these lines (WT: 0.035 ± 0.005 vs. pNAA10$^{R4S/Y}$: 0.071 ± 0.008, and eNAA10$^{R4S/Y}$: 0.064 ± 0.006; n = 15, 18, and 26, independent experiments; three independent differentiation experiments; $p = 0.0003$; Kruskal-Wallis test).

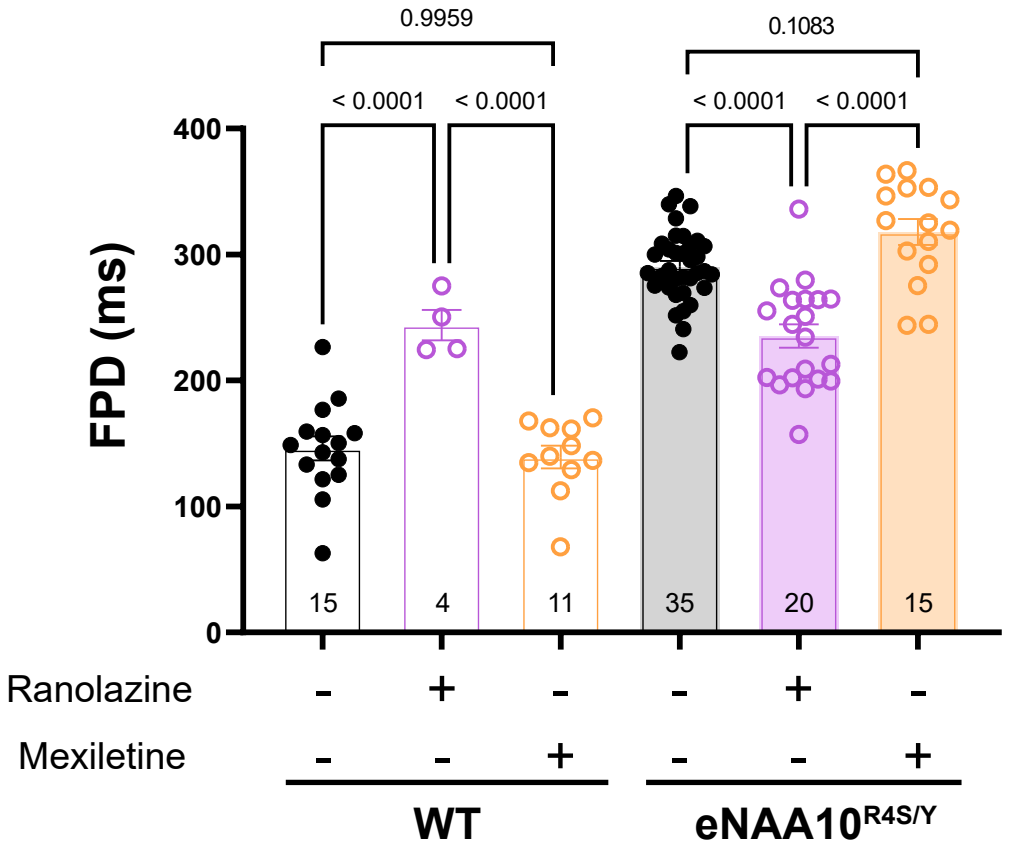

Supplementary Figure 11. Drug testing on microelectrode array. Ranolazine (100 μM) was administered. FPD was shortened in eNAA10$^{R4S/Y}$-iPSC-CMs, while it was prolonged in WT-iPSC-CMs. In contrast, Mexiletine (10 μM) had no significant effect on FPD in eNAA10$^{R4S/Y}$-iPSC-CMs. Data are presented as mean ± SEM from three independent differentiation experiments; statistical analysis was performed using one-way ANOVA. The number of cells is annotated on each graph.

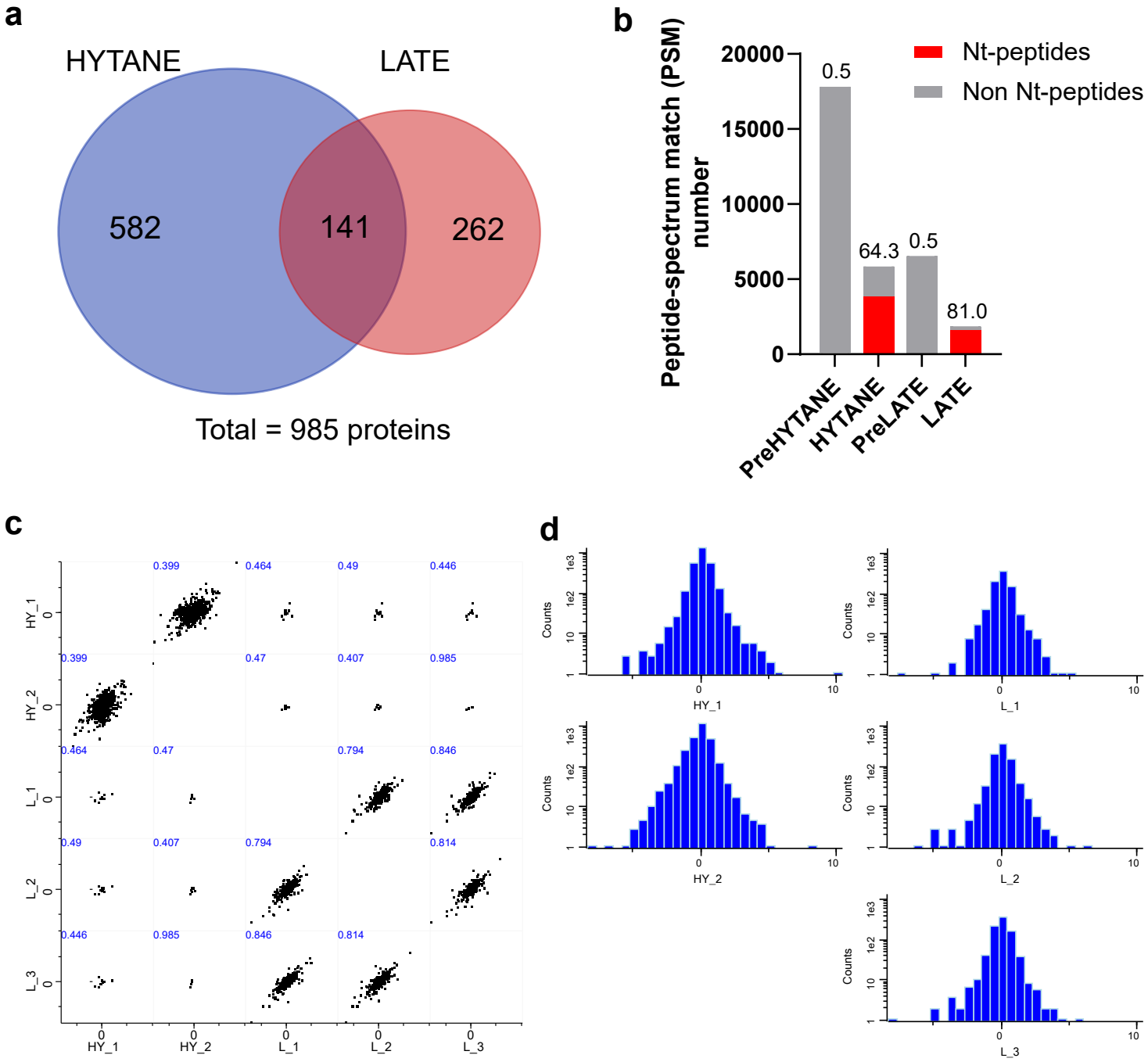

Supplementary Figure. 12. Proteomic analysis for iPSC-CMs. a. N-terminally acetylated proteins identified with HYTANE and LATE methods. A total of 985 proteins were identified. **b.** Peptide-spectrum match (PSM) number of N-terminal peptides (Nt-peptides) (red) and non Nt-peptides (gray) in pre-HYTANE, HYTANE, pre-LATE and LATE. HYTANE and LATE efficiently enriched Nt-peptides. The numbers on the bars denote the percentage of Nt-peptides. **c.** Multi-scatter plot of the pre-HYTANE samples and pre-LATE samples, showing a medium to high degree of correlation between the samples. **d.** Histogram showing the normal distributions of the H/L ratio. HYTANE: hydrophobic tagging-assisted N-termini enrichment; LATE: LysN amino terminal enrichment.

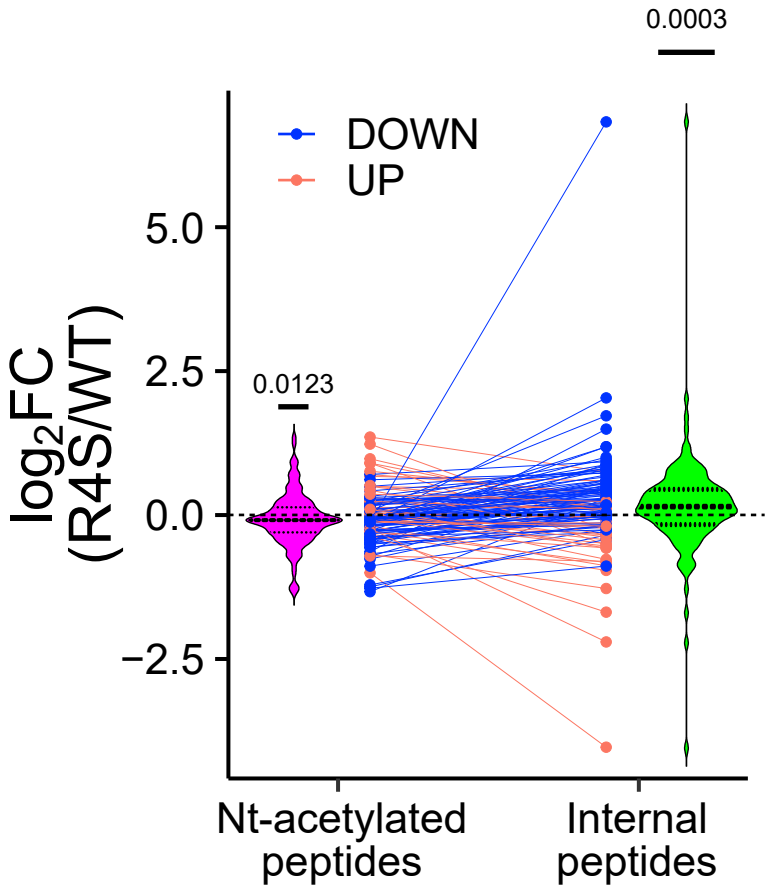

Supplementary Figure 13. Relationships between Nt-acetylated peptides and internal peptides in NatA proteins. Log_2 fold change (FC) of Nt-peptides and internal peptides from the same proteins was visualized with connecting lines. DOWN (blue) indicates proteins in which the relative ratio of Nt-acetylated peptides was downregulated, while UP (pink) indicates those in which it was upregulated. The violin plot (left, magenta) shows the log_2FC of Nt-peptides indicating a significant reduction in R4S (-0.076 ± 0.039; p = 0.0123; one-sample Wilcoxon test) while the right violin plot (green) shows the log2FC of internal peptides indicating significant increase in R4S (0.17 ± 0.079; p = 0.0003; one-sample Wilcoxon test).

Supplementary Table 1. Gating Parameters of NaV1.5 and CaV1.2 in WT- and NAA10$^{R4S/Y}$-iPSC-CMs.

I_{Na} parameters	WT	pNAA10$^{R4S/Y}$	eNAA10$^{R4S/Y}$	p-value
Peak I_{Na} density	-103.1 ± 9.8 (n = 14)	-271.6 ± 19.8** (n = 8)	-249.5 ± 30.8** (n = 10)	0.0017
Steady-state activation				
$V_{1/2}$	-21.6 ± 0.7	-26.8 ± 1.2*	-25.8 ± 0.8*	0.0275
k	6.5 ± 0.2	6.5 ± 0.2	6.9 ± 0.6	0.6465
Steady-state inactivation				
$V_{1/2}$	-69.0 ± 0.9	-77.4 ± 0.8**	-75.6 ± 0.8**	0.0010
k	6.7 ± 0.1	7.0 ± 0.2	6.6 ± 0.1	0.4684
$I_{Ca\text{-}L}$ parameters	**WT**	**pNAA10$^{R4S/Y}$**	**eNAA10$^{R4S/Y}$**	**p-value**
Peak $I_{Ca\text{-}L}$ density	-7.0 ± 1.2 (n = 3)	-6.4 ± 0.5 (n = 8)	-9.8 ± 1.1 (n = 6)	0.1492
Steady-state activation				
$V_{1/2}$	-6.8 ± 2.4	-10.2 ± 0.8	-10.9 ± 1.6	0.3246
k	8.7 ± 0.8	6.9 ± 0.4	6.7 ± 0.4	0.0918
Steady-state inactivation				
$V_{1/2}$	-40.1 ± 1.5	-41.5 ± 1.6	-46.9 ± 0.9	0.0317
k	7.9 ± 1.8	6.6 ± 0.1	6.5 ± 0.6	0.8453

Note: p-values were calculated using one-way ANOVA or Kruskal-Wallis test. * $p < 0.05$, **$p < 0.01$; Dunnett's multiple comparisons test for pNAA10$^{R4S/Y}$ or eNAA10$^{R4S/Y}$ versus WT.